HHS Public Access

Author manuscript

Nat Cell Biol. Author manuscript; available in PMC 2012 April 01.

Published in final edited form as:

Nat Cell Biol. ; 13(10): 1189–1201. doi:10.1038/ncb2328.

Apicobasal domain identities of expanding tubular membranes depend on glycosphingolipid biosynthesis

Hongjie Zhang[1], **Nessy Abraham**[1], **Liakot A. Khan**[1], **David H. Hall**[2], **John T. Fleming**[1], and **Verena Gobel**[1]

[1]Department of Pediatrics, Massachusetts General Hospital and Harvard Medical School, Boston, Massachusetts 02114, USA

[2]Center for C. elegans Anatomy, Department of Neuroscience, Albert Einstein College of Medicine, Bronx, New York 10461, USA

Abstract

Metazoan internal organs are assembled from polarized tubular epithelia that must set aside an apical membrane domain as a lumenal surface. In a global *Caenorhabditis elegans* tubulogenesis screen, interference with several distinct fatty-acid-biosynthetic enzymes transformed a contiguous central intestinal lumen into multiple ectopic lumens. We show that multiple-lumen formation is caused by apicobasal polarity conversion, and demonstrate that *in situ* modulation of lipid biosynthesis is sufficient to reversibly switch apical domain identities on growing membranes of single postmitotic cells, shifting lumen positions. Follow-on targeted lipid-biosynthesis pathway screens and functional genetic assays were designed to identify a putative single causative lipid species. They demonstrate that fatty-acid biosynthesis affects polarity via sphingolipid synthesis, and reveal ceramideglucosyltransferases (CGTs) as endpoint biosynthetic enzymes in this pathway. Our findings identify glycosphingolipids (GSLs), CGT products and obligate membrane lipids, as critical determinants of *in vivo* polarity and suggest they sort new components to the expanding apical membrane.

Original inquiries into intrinsic polarizing components of membrane biogenesis[1] were superseded by the characterization of specific membrane-associated polarity molecules: (1) plasma-membrane- and junction-associated protein complexes defining domain identities (identified by genetic morphogenesis screens in lower organisms); and (2) endomembrane-based sorting signals directing transport (identified by the analysis of trafficking in mammalian cell lines[2, 3]). It is unclear how these distinct polarizing cues are integrated, how

---

Correspondence and requests for materials should be addressed to VG (gobel@helix.mgh.harvard.edu)..

AUTHOR CONTRIBUTION: H. Z. generated and assembled most of the data and contributed to project design, data analysis and writing of the manuscript. N. A. participated in most experiments, performed the glycosylation screen and contributed to experimental design and data analysis. L. K. contributed to the genetic interaction experiments. D. H. H. and J. T. F. contributed to electron microscopy experiments and J. T. F. to writing of the manuscript. V. G. conceived and directed the project, participated in experiments and wrote the manuscript.

SUPPLEMENTAL INFORMATION Supplemental Information includes Methods and associated references, 8 figures, and 5 tables.

they themselves are regulated, and how they relate to other polarity cues that arise during cell division, migration and tissue morphogenesis[4, 5].

The limitation of genetic screens to identifying protein- or RNA-encoding genes may explain why lipids escaped numerous genetic screens instrumental in discovering *in vivo* core polarity determinants[6, 7]. In contrast, membrane lipids, particularly phosphoinositides, are well-established *in vitro* sorting signals[8–10]. GSLs, like phosophoinositides, are ubiquitous, asymmetrically assorted endo- and plasma-membrane lipids, but their polarity function is less clear *in vitro* and unknown *in vivo*. GSLs (with and without cholesterol) are thought to laterally self-assemble into membrane microdomains (rafts), and as such were implicated in the apical delivery of several molecules, particularly glycosylphosphatidylinositol(GPI)-anchored proteins, in mammalian cell lines[11–15]. A more general GSL role in partitioning apical proteins and lipids along endomembranes, originally proposed to generate polarity by segregating the GSL-rich apical plasma membrane domain, has not yet been demonstrated[16–18]. Studies are furthermore limited by uncertain effects of toxins and lipids used for the *in vitro* analysis of spingolipids. Additionally, GSL-biosynthetic-enzyme knockouts, although demonstrating an essential GSL role *in vivo*, failed to confirm a polarity function[19]. GSLs' ability to generate polarized plasma membrane domains is therefore uncertain and their essential role in development unknown.

Here, a global *C. elegans* tubulogenesis screen, followed by targeted lipid-biosynthetic pathway screens, identifies GSLs, the CGT products, as a lipid species, whose loss, along with each of ten of its upstream biosynthetic enzymes, displaces apical domains on expanding membranes, generating multiple intestinal lumens. An unbiased genetic morphogenesis screen thus identifies a membrane lipid with an apical sorting function in mammalian cell lines as an apical domain identity cue during *de novo* membrane biogenesis of invertebrate tubular epithelia.

RESULTS

Interference with four distinct lipid-biosynthetic enzymes converts apicobasal polarity, generating lateral lumens

To examine tubulogenesis and lumen formation, a visual RNA interference (RNAi) screen was performed using *C. elegans* engineered with ERM-1: :GFP-labeled lumenal membranes (Methods). RNAi with all chromosome III genes (N=2278) revealed that most (>90%) informative phenotypes involved essential genes, to which further genome screening was then restricted. A highly penetrant intestinal polarity phenotype (Fig.1a) was identified by knockdowns of each of four different lipid-biosynthetic enzymes: POD-2, an acetyl-CoA-carboxylase/ACC; LET-767, a steroid-dehydrogenase/3-ketoacyl-CoA-reductase/KAR; ACS-1, a long-chain-fatty-acid-acyl-CoA ligase; SPTL-1, a serine-palmitoyl-transferase/SPT. Single-cell analysis of intestinal tubulogenesis revealed the same sequence of events in all: in either late-stage embryos (*pod-2[RNAi]*) or first-stage larvae (L1; *let-767*, *acs-1*-, *sptl-1[RNAi]*, their respective arrest stages) ERM-1: :GFP decreased from the apical membrane and increased at basolateral membranes; lateral membranes transformed into ring structures; initially contiguous central apical ERM-1: :GFP fractionated into non-contiguous

lateral openings, suggesting multiple lateral ectopic lumens (Fig.1b, Fig.S1a,b). Digestive tract morphogenesis appeared otherwise unaffected and the epithelium intact (Fig.S2).

Additional apical submembraneous and integral membrane proteins were all similarly displaced to lateral membranes or the cytoplasm, including cortical actin and the apical Par(partitioning-defective)-polarity-complex component PAR-6. Basolateral molecules, including the polarity determinant LET-413/Scribble, were less affected, although partially displaced subapically (Fig.2a–h, Fig.S3a–d). Transmission-electron microscopy (TEM) revealed corresponding structural conversions of apical and basolateral domains: microvilli and the submembraneous terminal web were lost apically and acquired laterally, identifying lateral openings as true lumens rather than membrane adhesion defects or intracellular vacuoles (Fig.1c, Fig.S1c,S3h).

Apicobasal polarity defects of developing epithelia have been characterized as polarity loss through membrane equilibration and as unilateral, typically apical, domain expansion; both changes generally caused by apical junction defects[3, 7]. In contrast, we find polarity conversion: apical characteristics are coincidentally lost from the original apical, and gained by the original lateral domain. In further contrast, intestines lacked typical apical junction defects[20]: loss, fragmentation or displacement of AJM-1, HMP-1/Alpha-catenin, DLG-1/Discs-large from apicolateral junctures; ultrastructural defects at apicolateral sealing positions; label uptake from fluorescently-labeled bacterial food into intercellular spaces. Conversely, after polarity conversion but before single lateral lumen formation, additional junctions formed between nascent lateral lumens, suggesting they contribute to *de novo* apical domain biogenesis on the lateral side rather than reflecting an assembly defect preceding and causing the polarity alteration (Fig.1c, Fig.2i–k, Fig.S3e–h).

We conclude that interference with any one of four distinct lipid-biosynthetic enzymes converts intestinal apicobasal membrane domain identities, generating separate lateral lumens.

Lipid-biosynthetic enzymes affect apical sorting during *de novo* membrane biogenesis

C. elegans intestinal cell division, migration and intercalation are complete at mid-embryogenesis. To test if the late-embryonic or larval polarity changes reflected a role of lipid-biosynthetic enzymes in polarity maintenance rather than establishment, enzymes were RNAi-inactivated post-embryogenesis (Methods). This was sufficient to displace ERM-1::GFP basolaterally and switch lumen position in the mature larval, but not adult, epithelium (Fig.S4a). Lipid-biosynthetic enzymes thus maintain postmitotic intestinal polarity, but only in larvae, not in adults (a potential early embryonic requirement, e. g. via maternal lipids, cannot be excluded).

The morphogenetic feature distinguishing larval from adult intestines is net growth[21], suggesting that lipid-biosynthetic enzymes' polarity function was linked to epithelial expansion. Consistent with this, full polarity conversion, although confined to one stage (the arrest stage: late embryo or L1), required an extended period of time where animals grow (~two days at 20°C; Fig.3a). Notably, growth suppression via food deprivation[22] attenuated it, indicating that membrane expansion was required to manifest the polarity change

(Fig.S4b–c). To explore the role of lipid-biosynthetic enzymes in *de novo* polarized membrane biogenesis, we searched for a newly apically-delivered polarized molecule that was laterally displaced upon lipid-biosynthesis perturbations. ERM-1: :GFP recovery after *erm-1(RNAi)* removal revealed that ERM-1 is continuously supplied to larval, but not adult, lumenal membranes (peak delivery in L1s; Fig.S5). Since ERM-1: :GFP is displaced from expanding, but not non-expanding (starved) larval or adult membranes, these enzymes must target new components to the apical membrane during its biogenesis.

If lipid-biosynthetic enzymes maintain polarity by sorting newly-synthesized membrane components, the effect of their loss might be reversible. To test this, their activity was restored in enzyme-depleted RNAi larvae with ectopic lumens. Strikingly, lipid-biosynthesis reactivation reversed apical membrane lateralization, closed lateral lumens, rebuilt a contiguous central lumen and rescued growth-arrest and lethality (Fig.3b; FigS4b–d for comparison to Dauer-dependent arrest reversal).

We conclude that specific components of lipid biosynthesis are required to sort apical molecules during *de novo* membrane biogenesis, sustaining apicobasal domain identities and a contiguous lumen in *C. elegans* intestinal epithelia.

Polarized membrane biogenesis requires saturated long-chain-fatty-acid (LCFA) biosynthesis

We considered that *pod-2-*, *let-767-*, *acs-1-* and *sptl-1(RNAi)*-induced polarity defects might result from the loss of a common single lipid product, although these enzymes were not components of an obvious biosynthetic pathway. We first examined POD-2, LET-767 and ACS-1, all biochemically defined fatty-acid-biosynthetic enzymes with intestinal localization[23–25]. Knockdowns were validated as specific and severe losses-of-functions by confirming ERM-1: :GFP displacement in *pod-2(ye60)* intestines[25] (not shown) and demonstrating increasing polarity and tubulogenesis defects in an allelic series of *let-767* loss-of-function mutants[26] (Fig.4a–b).

Disrupting biosynthetic pathways increases upstream substrates while decreasing downstream products. It was thus unlikely that toxic intermediates would induce polarity defects generated by losing different enzymes, including one catalyzing the first committed step in *de novo* lipid biosynthesis (POD-2). Confirming this, exogenous fatty acids rescued the phenotype, in addition to the previously demonstrated wild-type gene rescue[23,25] (Fig. 4c–d). This result also excluded non-lipid-related dual enzyme functions and supported the assumption that losing one or more lipid compounds generated the phenotype.

Next, we knocked down 162 genes known or predicted to contribute to fatty-acid biosynthesis, metabolism or transport. Animals were examined for tubular polarity defects and negative results confirmed in selected germline mutants at pathway branch-points (Fig. 5, Tab.S1). One additional enzyme was identified: ELO-3, an elongase predicted to generate LCFAs (Fig.5, Fig.S6a). ELO-3's identification supported the prior identification of POD-2, LET-767 and ACS-1, the former catalyzing the first step synthesizing short- and medium-length saturated fatty acids (SFAs; LCFA building blocks) and the latter directly

contributing to LCFA biosynthesis of straight or monomethyl-branched-chain fatty acids (mmBCFAs)[23, 24, 27].

Since elongases condense fatty acids to ketoacyl-CoA, ELO-3 might generate the substrate for the 3-ketoacyl-CoA reductase LET-767. To examine the enzymatic step downstream of this reductase we searched the *C.elegans* genome for an ortholog predicted to use the LET-767 product 3-hydroxy-acyl-CoA as a substrate and identified 3-hydroxyacyl-CoA dehydratase homology in the PTP-like protein T15B7.2. Its knockdown copied the phenotype (Fig.5, Fig.S6b), suggesting that ELO-3, LET-767 and T15B7.2 catalyze consecutive steps in the biosynthesis of the presumed polarity-affecting lipid.

In contrast, desaturase gene knockdowns did not generate the polarity defect. Desaturases synthesize mono- and polyunsaturated fatty acids (MUFAs and PUFAs)[28, 29]. This negative result was confirmed in the non-redundant strong loss-of-function allele *fat-2(wa17)* that lacks normal PUFAs[29] (Fig.5, not shown), although not additionally confirmed in germline mutants of redundant MUFA desaturases[28].

We conclude that a putative common lipid species should contain saturated LCFAs, possibly MUFAs, probably mmBCFAs, but not PUFAs, excluding many lipid-signaling molecules and phosphoinositides as candidates for this specific polarity function.

Saturated long-chain-fatty-acid biosynthesis determines polarity via sphingolipid synthesis

We next examined the fourth identified enzyme, SPTL-1, predicted to condense a fatty acid with serine to form the long-chain-base (LCB) sphinganine as the first committed step in *de novo* sphingolipid synthesis (Fig.6a,7a). As expected, fatty acids did not rescue its RNAi phenotype (Fig.4c). Sphingolipid's role in polarity was, however, confirmed via *sptl-1(RNAi)* phenocopy by: double knockdowns of *sptl-2* and *sptl-3*, two additional *C.elegans* SPTs (Fig.S6e); feeding Myriocin or Fumonisin B, mycotoxins specifically inhibiting SPT and ceramide synthase (CerS), respectively. Both inhibitors dose-dependently induced the phenotype (Fig.7a, Fig.S6c). Since CerS generates ceramide from sphinganine, we infer that sphinganine itself, previously suggested to affect polarity in hepatoma cell lines[30], is excluded here since both sphinganine loss (via Myriocin and *sptl-1[RNAi]*) and excess (via Fumonisin) generate the phenotype.

Ceramide (Cer), the building block of all complex sphingolipids, contains a second LCFA in addition to the one used for the LCB (Fig.6a). Sphingolipid synthesis is thus strictly dependent on LCFAs, generally SFAs, and, in *C.elegans*, mmBCFAs[31], but not PUFAs, making sphingolipids good candidates for the putative common lipid compound. A series of experiments supported this idea. First, *pod-2-*, *acs-1-* and *let-767(RNAi)* phenotypes failed to efficiently reverse when sphingolipid synthesis was inhibited (Fig.6b). Second, mild *sptl-1*, *pod-2* and *acs-1* RNAi enhanced moderate *let-767* alleles (not shown) and were themselves dominantly enhanced by *let-767(s2819)*;sDp3. Third, mass spectrometry (MS) profiles of selected sphingolipids showed similar reductions in *let-767*, *acs-1-* and *sptl-1(RNAi)* animals (Fig.6d–e, Tab.S3). These profiles also confirmed that *C. elegans* sphingolipids utilize C17 mmBCFAs for the LCB[31], and demonstrated that saturated LCFAs are used for the

ceramide. Finally, exogenous sphingolipids partially rescued the polarity phenotype of fatty-acid-biosynthetic-enzyme-deficient animals (see below).

We conclude that *pod-2*, *let-767*, *acs-1*, *elo-3* and T15B7.2 are *C. elegans* sphingolipid-biosynthesis pathway components, and as such required for tubular polarity. We also note that the essential but unknown mmBCFA function[27] at least partially results from contributing to polarity and tubulogenesis via sphingolipid synthesis.

Polarity depends on ceramideglucosyltransferases

To identify the putative common polarity-affecting sphingolipid species, we knocked down 85 genes predicted to contribute to complex lipid and sphingolipid metabolism and regulation, adding double and triple RNAi and RNAi-sensitive conditions to detect redundant enzymes and mild effects (Fig.7a, Tab.S2, Methods). The phenotype was found in the single knockdown of a predicted sphingolipid-fatty-acid hydroxylase, C25A1.5, and the double knockdown of the CGT orthologs *cgt-1* and *cgt-3* (Fig.S6d,f). CGTs only generate glucosylceramide (GlcCer), the GSL backbone[17], and, in contrast to the previously identified enzymes, do not produce substrates for the biosynthesis of multiple lipids. This result therefore identifies GSLs as the furthest downstream polarity-affecting lipid species, and suggests that their loss generates the polarity defects induced by its ten upstream lipid-biosynthetic enzymes.

Several findings further supported CGTs' and GSLs' role in tubular polarity. Prior studies determined that: *C. elegans'* CGTs are expressed and function cell-autonomously in the intestine; they synthesize GSLs *in vitro* and *in vivo*; arrested *cgt-1,ctg-3*-double and *cgt-1,ctg-2,ctg-3*-triple RNAi/mutant larvae have reduced although not absent GSL levels[32–35]. We found the polarity phenotype in double *cgt-1(tm999);cgt-3(tm504)* mutants, different combinations of *cgt-1*, *cgt-3*-double mutant/RNAi animals, and animals fed with the CGT inhibitor D,L-threo-PDMP (Fig.S6f–g, not shown; Methods). Although complex membrane lipids might not be expected to recapitulate their endogenous roles as endproducts on membranes[36] (in contrast, exogenous fatty acids can function as metabolic intermediates or signaling molecules[24, 25]; compare Fig.4c–d), exogenous labeled and unlabeled sphingolipids were tested for rescue. Neither we nor others could rescue *cgt-1;cgt-3*-double-mutant/RNAi-induced lethality with exogenous GSLs[34], however, feeding a mixture of synthetic sphingolipids (including GSLs), made to human templates, mildly improved *ctg-1(tm999);ctg-3(RNAi)* tubulogenesis defects, and C6-NBD-GlcCer uptake attenuated their severity (Fig.7b–c).

Without excluding other possible sphingolipid contributions, additional results suggested that GSLs mediate the polarity effect of their upstream fatty-acid- and sphingolipid-biosynthetic enzymes: moderate *cgt-1;cgt-3(RNAi)* polarity phenotypes were dominantly enhanced by *let-767(s2819)*;sDp3 (Fig.6c); *ctg-1(tm999);ctg-(RNAi)*-rescuing sphingolipids and GSLs likewise partially rescued *let-767*- and *sptl-1-(RNAi)* tubulogenesis defects that were similarly attenuated by C6-NBD-GlcCer (Fig.7b–c); MS profiles displayed comparable GSL losses in fatty-acid-and sphingolipid-biosynthesis-defective animals (Fig.S7a, Tab.S3). Of note, the complex membrane sphingolipids GSL and sphingomyelin [SM] ratio was

consistently altered, with a greater loss of GSLs, suggesting a corresponding change in membrane lipid composition (Fig.S7b).

We conclude that the furthest downstream lipid-biosynthetic pathway enzyme CGT, and its product GlcCer are required for tubular polarity, suggesting that GSLs are the polarity-affecting common lipid species.

Polarity requires hydroxylated glucosylceramide, while further sugar modifications are dispensable

GSLs could affect polarity via GlcCer intermediates, derivatives, or GlcCer itself. The pathway screen's systematic approach largely excludes the first: gaining and losing multiple different intermediates of eleven GSL-biosynthetic enzymes equally disturbs polarity. This includes ceramide, GlcCer's immediate metabolite (single and double RNAi of glucocerebrosidases also failed to generate the phenotype, although multiple-null mutants were not tested [Tab.S2]). Since GSL metabolism occurs on endomembranes[37], it cannot, however, be excluded that they function through an organelle-sequestered intermediate subfraction.

Further sugar modifications of GlcCer's backbone create the large GSL family[38]. Single knockdowns of 112 gene candidates for the biosynthesis or function of GlcCer-derivatives (Tab.S4), including those previously ordered into a biosynthetic pathway for insect-specific derivatives[39], failed to generate the polarity phenotype. *bre-3(ye26)*/ Beta4Mannosyltransferase, a viable, presumed null allele catalyzing the first step in their biosynthesis, confirmed these negative results, excluding the arthro-series of GlcCer-derivatives as required for this function (Fig.7d).

Our MS profile furthermore revealed the complete absence of lactosylceramide (LacCer) and consequently the entire GSL lacto-series (Fig.S7c–d), supporting previous assumptions that *C. elegans*, like *Drosophila*, exclusively uses the arthro-series of GlcCer-derivatives[39, 40]. In the absence of as-of-yet unidentified novel GSL sugar modifications, these results suggest that GlcCer itself exerts the polarity effect, for which additional sugar modifications are dispensable.

Finally, our MS analysis characterized GlcCer as invariably hydroxylated, consistent with the identified sphingolipid fatty-acid hydroxylase, C25A1.5, and containing a saturated LCFA of C21–C26 chain length, with C22 in greatest abundance (Fig.7e).

We conclude that the polarity-affecting lipid compound is likely GlcCer-OH itself, with or without specific sugar modifications, with a C17-branched-chain LCB and a saturated LCFA of length C21–C26, probably C22 (Fig. 7e inset).

GSL biosynthesis affects vesicular trafficking

GSLs localize to endothelial vesicleand lumenal-plasma membranes, are synthesized on vesicle membranes, and apically sort several membrane molecules in mammalian epithelial cell lines[8, 14, 41]. Feeding partially rescuing C5–BODIPY-Cer and C12-NBD-GlcCer

suggested that both lipids also localize to vesicles and the lumenal membrane of the *C. elegans* intestine (Fig.8a).

Consistent with a conserved GSL trafficking function were the following findings: low-temperature interference with trafficking suppressed the polarity conversion, suggesting vesicular transport was required to reveal the misdirection of apical membrane components (Fig.8b, Fig.S8a–g; note: low temperature also slows growth and development); *sptl-1(RNAi)* intestinal sections revealed vesicle paucity, along with distended endoplasmic reticular (ER) and Golgi membranes (Fig.8c, Fig.S8h–i); the *pod-2-*, *let-767-*, *acs-1-*, *sptl-1(RNAi)* and *cgt-1(tm999)/cgt-3(RNAi)*-induced polarity conversion depleted intestinal endosomes, primarily RAB-11-associated, presumed lumenal-membrane-forming vesicles[4, 42] (Fig.8d, not shown). RAB-11-positive vesicles were first slightly enlarged, then lost from the apical membrane; RAB-5-associated early endosomes were occasionally mildly enlarged subapically; L1-specific RAB-7-positive apical clusters, but not the presumed Golgi-associated mid-cytoplasmic endosomes, were decreased in number or absent; RAB-10-associated basolateral recycling endosomes were least affected[43]. Alpha-mannosidaseII(MANS)-associated Golgi membranes, distributed as mini-stacks throughout the wild-type *C. elegans* cytoplasm[43, 44], contracted basolaterally, assuming a linear, possibly tubulated, pattern (Fig.8d).

Finally, C5–BODIPY-Cer and C12-NBD-GlcCer, which only mildly improve polarity defects, were themselves displaced to lateral ectopic lumenal membranes in *sptl-1(RNAi)* and *cgt-1(tm999)/cgt-3(RNAi)* intestines (Fig.8e), demonstrating that GSL biosynthesis also affects the targeting of lipids, including its own apical placement. Given GSLs' obligate membrane association, this finding further supports a function of GSL biosynthesis in the vesicular delivery of apically-destined molecules during membrane biogenesis.

DISCUSSION

GSLs' long-proposed essential role in development has remained mysterious, and their postulated contribution to *in vivo* polarity uncertain[14, 19, 45, 46]. Here, an unbiased genetic tubulogenesis screen uncovers an essential role for GSLs in maintaining polarity and a central lumen in the developing *C. elegans* intestine. Our analysis suggests that endoand plasma-membrane-associated GSLs determine polarity by sorting new components to expanding apical membranes: (1) their loss simultaneously decreases molecular and structural apical characteristics at original apical membranes while increasing them at original lateral membranes; (2) this polarity conversion diverts newly-synthesized membrane components from their apical path; (3) it requires cell growth and trafficking, but not cell division, migration or junction disassembly; (4) it is reversible in single cells upon restoration of lipid biosynthesis; (5) it depletes apical endosomes, including RAB-11-associated lumenal vesicles; (6) it affects GSLs' own presumed membrane-associated apical delivery. Without excluding additional GSL roles in structural membrane biogenesis or other trafficking aspects, an apical sorting function is strongly supported by GSLs' documented *in vitro* ability to deliver several apical molecules[8, 11, 12, 15]. Our findings in turn now provide evidence for the relevance of these *in vitro* findings for polarized tissue morphogenesis *in vivo*, and for the proposition that GSLs could determine apical plasma

membrane domain identity[47]. GSLs, like phosphoinositides, may combine aspects of both endo- and plasma-membrane-based polarity cues, suggesting a mode of integration for these distinct membrane-associated polarity determinants[2]. Phosphoinositides, classical vesicle-based sorting signals[9], do, in fact, control plasma membrane domain identity and affect mammalian tubulogenesis *in vitro*.[5, 48, 49]

Previously characterized core polarity determinants of developing epithelia, such as the Par-, Crumbs-, and Scribble-related protein complexes, were characterized in proliferating and migrating cells or cell populations[2, 3, 7]. Our *in vivo* single-cell analysis of postmitotic expanding epithelia, that separated membrane biogenesis from proliferation- and migration-dependent polarity cues, may have allowed the identification of these structural membrane lipids' innate sorting ability during *de novo* membrane biogenesis. This analysis also revealed unanticipated aspects of polarity and tissue plasticity: polarity remains dynamic in single postmitotic cells; the lumen position is flexible in a fully constructed tube epithelium; and both polarity and lumen position can be reversibly shifted on the growing membrane *in situ* by lipid-biosynthesis modulation. How could GSLs sort lumenal membrane components? GSLs' sorting function in mammalian cell lines was linked to the formation of rafts, thought to form on lumenal vesicle- and plasma-membrane leaflets[10, 50, 51]. However, GLcCer, the GSL backbone without sugar modification, is uniquely placed on cytoplasmic membrane leaflets, a location distinct from its derivatives and of unknown significance[14]. Here it could directly interact with apically-destined cytoplasmic molecules, polarity determinants, or coat complexes. Intriguingly, loss of *tat-2*, a *C. elegans* flippase that vertically translocates lipids between membrane leaflets, rescues the lethality of *sptl-1* and mmBCFAs loss[52]. If TAT-2 were to flip GlcCer to the lumenal leaflet, its loss would increase GlcCer at the cytoplasmic leaflet where it could improve apical transport. A GSL-specific flippase was postulated, but not yet identified[14, 17].

While GlcCer sugar modifications are deemed critical for sorting in mammalian cell lines[8] (a finding unconfirmed by their biosynthetic enzymes' targeted deletions in mice[19]), we found it dispensable for tubular polarity *in vivo*. The vertebrate- and invertebrate-specific lactose- and arthro-series of GlcCer-derivatives can be swapped in *Drosophila* for developmental functions[53], suggesting tolerance for sugar modifications, emphasizing the sphingolipid backbone's importance, and further supporting its interspecies conserved function. In intriguing agreement with our findings, epithelial polarization in mammalian cell lines was recently linked to GSL glycans[54], and to an SM-to GSL-biosynthesis switch, with an increase in GSL fatty-acid length, saturation and hydroxylation[55].

GlcCer (or GlcCer-OH), as part of complex GSLs, could also affect sorting via lipid-lipid-microdomain or lipid-protein-shell formation on lumenal membrane leaftlets[18, 50, 51]. Our finding that GSL biosynthesis positions the apical domain during *de novo* membrane biogenesis is unexpectedly consistent with the original, but subsequently abandoned, proposition that GSLs segregate the apical plasma membrane via endomembrane maturation during bulk membrane biogenesis[16]. GSLs' dose-dependent effect on polarity and the rescue of moderate GSL-dependent polarity defects by growth restriction, suggest that GSLs' relative proportions are critical for polarized membrane biogenesis. The dependency of GSLs' apical placement on their own biosynthesis is consistent with a requirement for their

endomembrane-associated synthesis, a scenario compatible with the proposed polarizing component of membrane biogenesis by lipid-based self-organization[16].

Despite known functions in polarized morphogenesis *in vitro*[48, 49], lipids escaped identification in numerous genetic polarity screens. Lipid-biosynthetic enzymes identified in genetic screens are often not pursued since they typically synthesize multiple compounds. Here we show that systematic biosynthetic pathway targeting, combined with genetic interaction studies, can identify an endpoint biosynthetic enzyme, and thus a lipid species. Along with defining biosynthesis pathways (here, the *C. elegans* sphingolipid biosynthesis pathway), this approach can identify multiple proteins directly controlling a function of interest (here, eleven lipid-biosynthetic enzymes directly regulating tubular polarity), and may reveal novel functions of intermediates (here, the enigmatic mmBCFAs' role in tubular polarity). Notably, the simultaneous generation of multiple loss- and gain-of-function conditions for downstream products and upstream substrates, respectively, inherent to this approach, helps distinguish primary from secondary changes, a particular conundrum of lipid analysis where intermediates are interconverted and compensatory changes frequent[56]. The additional biosynthetic screen for sugar modifications demonstrated that an identified lipid species can be further defined as a chemical compound and suggests that such screens can also be used for the analysis of sugars. This approach should be generally applicable to extend the power of unbiased genetic screens to non-proteinaceous compounds, identifying their *in vivo* cellular roles beyond known metabolic functions.

METHODS

Methods and any associated references are available in the online version of the paper at http://www.nature.com/naturecellbiology/.

Supplementary Material

Refer to Web version on PubMed Central for supplementary material.

ACKNOWLEDGEMENTS

Strains and plasmids were kindly provided by D. Baillie, A. Croce, B. Grant, K. Kemphues, K. Nehrke, G. Ruvkun, K. Strange, J. Simske, and by S. Mitani, National Bioresource Project Japan, and by the Caenorhabditis Genetics Center (NIH Center for Research Resources). We thank G. Ruvkun for the lethal RNAi library, and J. Moore (Avanti Polar Lipids); Mary McKee (MGH Microscopy Core/partially funded by the IBD grant DK43351 and BA DE award DK57521) and K. Nygen; Christopher Crocker; and Edward Membreno for contributions to LC/MS; TEM; illustrations and *C. elegans* maintenance, respectively. We thank F. Solomon and B. Winckler for critical reading of the manuscript and H. Weinstein and A. Walker for ongoing support. This work was supported by NIH grants HD044589 and GM078653 to VG.

REFERENCES

1. Pfeffer SR, Rothman JE. Biosynthetic protein transport and sorting by the endoplasmic reticulum and Golgi. Annu Rev Biochem. 1987; 56:829–852. [PubMed: 3304148]
2. Mellman I, Nelson WJ. Coordinated protein sorting, targeting and distribution in polarized cells. Nat Rev Mol Cell Biol. 2008; 9:833–845. [PubMed: 18946473]
3. St Johnston D, Ahringer J. Cell polarity in eggs and epithelia: parallels and diversity. Cell. 141:757–774. [PubMed: 20510924]

4. Bryant DM, et al. A molecular network for de novo generation of the apical surface and lumen. Nat Cell Biol. 12:1035–1045. [PubMed: 20890297]
5. Martin-Belmonte F, Rodriguez-Fraticelli AE. Chapter 3: acquisition of membrane polarity in epithelial tube formation patterns, signaling pathways, molecular mechanisms, and disease. Int Rev Cell Mol Biol. 2009; 274:129–182. [PubMed: 19349037]
6. Kemphues KJ, Priess JR, Morton DG, Cheng NS. Identification of genes required for cytoplasmic localization in early C. elegans embryos. Cell. 1988; 52:311–320. [PubMed: 3345562]
7. Nelson WJ. Adaptation of core mechanisms to generate cell polarity. Nature. 2003; 422:766–774. [PubMed: 12700771]
8. Rodriguez-Boulan E, Kreitzer G, Musch A. Organization of vesicular trafficking in epithelia. Nat Rev Mol Cell Biol. 2005; 6:233–247. [PubMed: 15738988]
9. Di Paolo G, De Camilli P. Phosphoinositides in cell regulation and membrane dynamics. Nature. 2006; 443:651–657. [PubMed: 17035995]
10. Lippincott-Schwartz J, Phair RD. Lipids and cholesterol as regulators of traffic in the endomembrane system. Annu Rev Biophys. 39:559–578. [PubMed: 20192772]
11. Mays RW, et al. Hierarchy of mechanisms involved in generating Na/K-ATPase polarity in MDCK epithelial cells. J Cell Biol. 1995; 130:1105–1115. [PubMed: 7657695]
12. Sprong H, et al. Glycosphingolipids are required for sorting melanosomal proteins in the Golgi complex. J Cell Biol. 2001; 155:369–380. [PubMed: 11673476]
13. Hoekstra D, Maier O, van der Wouden JM, Slimane TA, van ISC. Membrane dynamics and cell polarity: the role of sphingolipids. J Lipid Res. 2003; 44:869–877. [PubMed: 12639977]
14. Degroote S, Wolthoorn J, van Meer G. The cell biology of glycosphingolipids. Semin Cell Dev Biol. 2004; 15:375–387. [PubMed: 15207828]
15. Mayor S, Riezman H. Sorting GPI-anchored proteins. Nat Rev Mol Cell Biol. 2004; 5:110–120. [PubMed: 15040444]
16. Simons K, van Meer G. Lipid sorting in epithelial cells. Biochemistry. 1988; 27:6197–6202. [PubMed: 3064805]
17. van Meer G, Voelker DR, Feigenson GW. Membrane lipids: where they are and how they behave. Nat Rev Mol Cell Biol. 2008; 9:112–124. [PubMed: 18216768]
18. Lingwood D, Simons K. Lipid rafts as a membrane-organizing principle. Science. 327:46–50. [PubMed: 20044567]
19. Furukawa K, Tokuda N, Okuda T, Tajima O. Glycosphingolipids in engineered mice: insights into function. Semin Cell Dev Biol. 2004; 15:389–396. [PubMed: 15207829]
20. Lynch AM, Hardin J. The assembly and maintenance of epithelial junctions in C. elegans. Front Biosci. 2009; 14:1414–1432.
21. Knight CG, Patel MN, Azevedo RB, Leroi AM. A novel mode of ecdysozoan growth in Caenorhabditis elegans. Evol Dev. 2002; 4:16–27. [PubMed: 11871396]
22. Baugh LR, Sternberg PW. DAF-16/FOXO regulates transcription of cki-1/Cip/Kip and repression of lin-4 during C. elegans L1 arrest. Curr Biol. 2006; 16:780–785. [PubMed: 16631585]
23. Entchev EV, et al. LET-767 is required for the production of branched chain and long chain fatty acids in Caenorhabditis elegans. J Biol Chem. 2008; 283:17550–17560. [PubMed: 18390550]
24. Kniazeva M, Euler T, Han M. A branched-chain fatty acid is involved in post-embryonic growth control in parallel to the insulin receptor pathway and its biosynthesis is feedback-regulated in C. elegans. Genes Dev. 2008; 22:2102–2110. [PubMed: 18676815]
25. Rappleye CA, Tagawa A, Le Bot N, Ahringer J, Aroian RV. Involvement of fatty acid pathways and cortical interaction of the pronuclear complex in Caenorhabditis elegans embryonic polarity. BMC Dev Biol. 2003; 3:8. [PubMed: 14527340]
26. Kuervers LM, Jones CL, O'Neil NJ, Baillie DL. The sterol modifying enzyme LET-767 is essential for growth, reproduction and development in Caenorhabditis elegans. Mol Genet Genomics. 2003; 270:121–131. [PubMed: 12905072]
27. Kniazeva M, Crawford QT, Seiber M, Wang CY, Han M. Monomethyl branched-chain fatty acids play an essential role in Caenorhabditis elegans development. PLoS Biol. 2004; 2:E257. [PubMed: 15340492]

28. Brock TJ, Browse J, Watts JL. Fatty acid desaturation and the regulation of adiposity in Caenorhabditis elegans. Genetics. 2007; 176:865–875. [PubMed: 17435249]
29. Watts JL, Browse J. Genetic dissection of polyunsaturated fatty acid synthesis in Caenorhabditis elegans. Proc Natl Acad Sci U S A. 2002; 99:5854–5859. [PubMed: 11972048]
30. Van ISC, Van Der Wouden JM, Liebisch G, Schmitz G, Hoekstra D. Polarized membrane traffic and cell polarity development is dependent on dihydroceramide synthase-regulated sphinganine turnover. Mol Biol Cell. 2004; 15:4115–4124. [PubMed: 15229289]
31. Chitwood DJ, Lusby WR, Thompson MJ, Kochansky JP, Howarth OW. The glycosylceramides of the nematode Caenorhabditis elegans contain an unusual, branched-chain sphingoid base. Lipids. 1995; 30:567–573. [PubMed: 7651085]
32. Ichikawa S, Hirabayashi Y. Glucosylceramide synthase and glycosphingolipid synthesis. Trends Cell Biol. 1998; 8:198–202. [PubMed: 9695839]
33. Leipelt M, et al. Glucosylceramide synthases, a gene family responsible for the biosynthesis of glucosphingolipids in animals, plants, and fungi. J Biol Chem. 2001; 276:33621–33629. [PubMed: 11443131]
34. Marza E, Simonsen KT, Faergeman NJ, Lesa GM. Expression of ceramide glucosyltransferases, which are essential for glycosphingolipid synthesis, is only required in a small subset of C. elegans cells. J Cell Sci. 2009; 122:822–833. [PubMed: 19240113]
35. Nomura KH, et al. Ceramide glucosyltransferase of the nematode Caenorhabditis elegans is involved in oocyte formation and in early embryonic cell division. Glycobiology. 21:834–848. [PubMed: 21325339]
36. Maier O, Oberle V, Hoekstra D. Fluorescent lipid probes: some properties and applications (a review). Chem Phys Lipids. 2002; 116:3–18. [PubMed: 12093532]
37. Hannun YA, Obeid LM. Principles of bioactive lipid signalling: lessons from sphingolipids. Nat Rev Mol Cell Biol. 2008; 9:139–150. [PubMed: 18216770]
38. Varki, A. Essentials of glycobiology. 2nd ed.. Cold Spring Harbor Laboratory Press; Cold Spring Harbor, N.Y.: 2009.
39. Griffitts JS, et al. Glycolipids as receptors for Bacillus thuringiensis crystal toxin. Science. 2005; 307:922–925. [PubMed: 15705852]
40. Gerdt S, Lochnit G, Dennis RD, Geyer R. Isolation and structural analysis of three neutral glycosphingolipids from a mixed population of Caenorhabditis elegans (Nematoda:Rhabditida). Glycobiology. 1997; 7:265–275. [PubMed: 9134433]
41. Futerman AH, Riezman H. The ins and outs of sphingolipid synthesis. Trends Cell Biol. 2005; 15:312–318. [PubMed: 15953549]
42. Weisz OA, Rodriguez-Boulan E. Apical trafficking in epithelial cells: signals, clusters and motors. J Cell Sci. 2009; 122:4253–4266. [PubMed: 19923269]
43. Chen CC, et al. RAB-10 is required for endocytic recycling in the Caenorhabditis elegans intestine. Mol Biol Cell. 2006; 17:1286–1297. [PubMed: 16394106]
44. Rolls MM, Hall DH, Victor M, Stelzer EH, Rapoport TA. Targeting of rough endoplasmic reticulum membrane proteins and ribosomes in invertebrate neurons. Mol Biol Cell. 2002; 13:1778–1791. [PubMed: 12006669]
45. Yamashita T, et al. A vital role for glycosphingolipid synthesis during development and differentiation. Proc Natl Acad Sci U S A. 1999; 96:9142–9147. [PubMed: 10430909]
46. Rao RP, Acharya JK. Sphingolipids and membrane biology as determined from genetic models. Prostaglandins Other Lipid Mediat. 2008; 85:1–16. [PubMed: 18035569]
47. Schuck S, Simons K. Polarized sorting in epithelial cells: raft clustering and the biogenesis of the apical membrane. J Cell Sci. 2004; 117:5955–5964. [PubMed: 15564373]
48. Gassama-Diagne A, et al. Phosphatidylinositol-3,4,5-trisphosphate regulates the formation of the basolateral plasma membrane in epithelial cells. Nat Cell Biol. 2006; 8:963–970. [PubMed: 16921364]
49. Martin-Belmonte F, et al. PTEN-mediated apical segregation of phosphoinositides controls epithelial morphogenesis through Cdc42. Cell. 2007; 128:383–397. [PubMed: 17254974]

50. Haucke V, Di Paolo G. Lipids and lipid modifications in the regulation of membrane traffic. Curr Opin Cell Biol. 2007; 19:426–435. [PubMed: 17651957]
51. Simons K, Gerl MJ. Revitalizing membrane rafts: new tools and insights. Nat Rev Mol Cell Biol. 11:688–699. [PubMed: 20861879]
52. Seamen E, Blanchette JM, Han M. P-type ATPase TAT-2 negatively regulates monomethyl branched-chain fatty acid mediated function in post-embryonic growth and development in C. elegans. PLoS Genet. 2009; 5:e1000589. [PubMed: 19662161]
53. Wandall HH, et al. Egghead and brainiac are essential for glycosphingolipid biosynthesis in vivo. J Biol Chem. 2005; 280:4858–4863. [PubMed: 15611100]
54. Mishra R, Grzybek M, Niki T, Hirashima M, Simons K. Galectin-9 trafficking regulates apical-basal polarity in Madin-Darby canine kidney epithelial cells. Proc Natl Acad Sci U S A. 107:17633–17638. [PubMed: 20861448]
55. Sampaio JL, et al. Membrane lipidome of an epithelial cell line. Proc Natl Acad Sci U S A. 108:1903–1907. [PubMed: 21245337]
56. Vance, DE.; Vance, JE. Biochemistry of lipids, lipoproteins and membranes (5th Edn.). 5th ed.. Elsevier; Amsterdam; London: 2008.
57. Gobel V, Barrett PL, Hall DH, Fleming JT. Lumen morphogenesis in C. elegans requires the membrane-cytoskeleton linker erm-1. Dev Cell. 2004; 6:865–873. [PubMed: 15177034]
58. Sulston JE, Horvitz HR. Post-embryonic cell lineages of the nematode, Caenorhabditis elegans. Dev Biol. 1977; 56:110–156. [PubMed: 838129]
59. Legouis R, et al. LET-413 is a basolateral protein required for the assembly of adherens junctions in Caenorhabditis elegans. Nat Cell Biol. 2000; 2:415–422. [PubMed: 10878806]
60. Kurzchalia TV, Ward S. Why do worms need cholesterol? Nat Cell Biol. 2003; 5:684–688. [PubMed: 12894170]
61. Martinez-Alonso E, Egea G, Ballesta J, Martinez-Menarguez JA. Structure and dynamics of the Golgi complex at 15 degrees C: low temperature induces the formation of Golgi-derived tubules. Traffic. 2005; 6:32–44. [PubMed: 15569243]
62. Onelli E, Prescianotto-Baschong C, Caccianiga M, Moscatelli A. Clathrin-dependent and independent endocytic pathways in tobacco protoplasts revealed by labelling with charged nanogold. J Exp Bot. 2008; 59:3051–3068. [PubMed: 18603619]

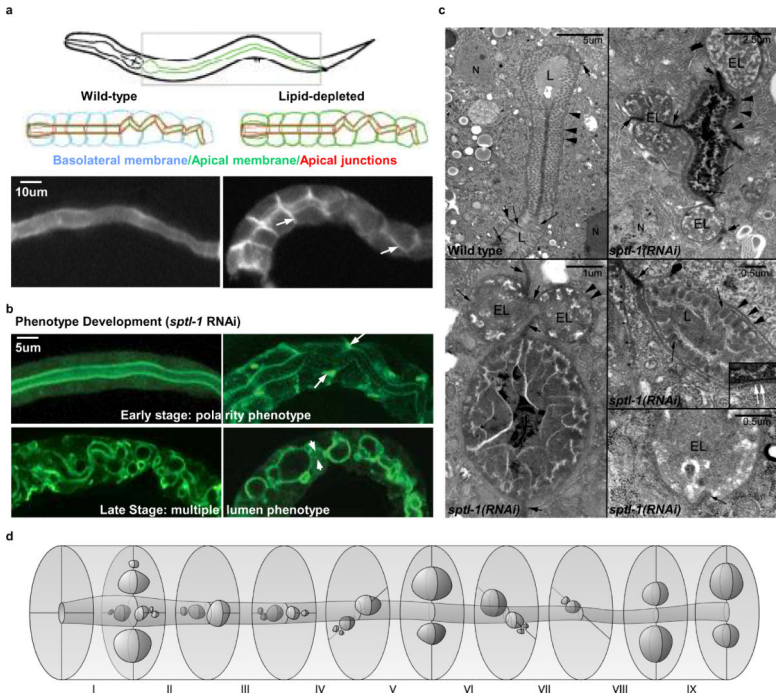

Figure 1. Apicobasal polarity conversion and ectopic lumen formation in the intestines of lipid-biosynthetic-enzyme-depleted animals (see Fig.S1 for anatomy and phenotypic details)

1**(a)** Top - Schematic of the mature single-layered *C. elegans* intestine where all apical membranes form the lumenal surface. Boxed area is magnified below. Bottom - Epifluorescent dissecting micrographs of live animals (as identified in screen) showing displacement of the membrane-cytoskeleton linker ERM-1: :GFP[57] from the apical = lumenal membrane in wild-type (left; for brevity, transgenic marker strains will be denoted as wild-type) to the basolateral membrane in lipid-biosynthetic-enzyme-depleted animal (right; left arrow: lateral side, right arrow: basal side; note wild-type intercalation pattern). Representative *sptl-1(RNAi)* L1 are shown; *pod-2-*, *let-767-*, *acs-1* RNAi copy the phenotype. (Fig.S1b). Here and below, standard RNAi conditions (Methods) are shown if not otherwise indicated; anterior is left and dorsal up. **(b)** Typical phenotype development in RNAi L1s. Confocal sections showing: initial wild-type ERM-1: :GFP placement (top left); ERM-1: :GFP reduction from apical, and displacement to basolateral, membranes and enrichment in apicolateral angles (arrows; top right); multiple small lateral ectopic lumens (bottom left); ERM-1: :GFP fully displaced from the central lumen to large lateral ectopic lumens (bottom right, arrows bracket central lumen area where ERM-1: :GFP is missing). **(c)** TEM micrographs of intestinal cross-sections of wild-type (top left) and *sptl-1(RNAi)* L1s (all others). Wild-type oval lumen (L) with dense microvilli (long black arrows) and tightly adjacent terminal web (arrowheads); deformed main lumen in RNAi animals with either short (long black arrows) or absent microvilli (right-middle inset, white arrows), dehiscence of the terminal web (arrowheads) and ectopic lateral lumens (EL) with stunted microvilli (long black arrows). Intact apical junctions (short arrows) in both wild type and RNAi animals; note excess junctions between ELs in RNAi animals; N, nucleus. Upper right image shows INT I. **(d)** Model of the multiple-lumen intestinal phenotype. Early ectopic lumen development (Fig.1b, bottom-left image) in otherwise wild-type intestine is shown.

Twenty intestinal cells are arranged in bilateral symmetry to form nine INT rings (I – IX; INT I contains four cells); rings twist along the anterior-posterior axis. View is from the anterior left lateral aspect[58].

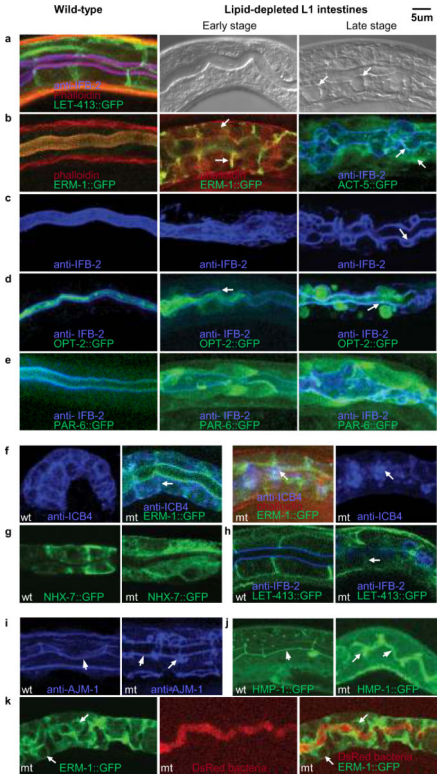

Figure 2. Apicobasolateral membrane and apical junction components in lipid-biosynthetic-enzyme-depleted intestines (Fig.S4 shows additional components)

(a – e) Apical membrane. (a) Left (L) to right (R): Confocal image of actin (phalloidin) overlay (purple) with intermediate filaments (IFB-2) at apical, and LET-413 at basolateral, membranes; Nomarski images: early phenotype lacks visible changes, later stage shows lateral lumens (arrows). (b) L to R: apical actin/ERM-1 overlay (yellow); displaced basolaterally (yellow, lower arrow) and cytoplasmically (red, upper arrow); cortical actin (ACT-5)/IFB-2 overlay displaced to lateralized lumenal membranes (turquoise, left arrow) and cytoplasm (green, right arrow). (c) L to R: apical submembraneous IFB-2; unraveling from lumen; displaced to lateralized lumenal membranes (arrow indicates central-lumenal IFB-2 contiguity). (d) L to R: OPT-2, a transmembraneous oligopeptide transporter, positioned apical to IFB-2 (green w/o overlay); displaced basolaterally (arrow); displaced lateral to lateralized IFB-2 (green w/o overlay; note displacement to, but not expansion into, the lateral domain [arrow]). (e) L to R: IFB2/PAR-6 overlay (turquois); cytoplasmic PAR-6 displacement at early and late stage (green). **(f – h)** Basolateral membrane. (f) L to R: ICB4 stains an unknown panmembraneous marker in wild-type (wt); apicobasolateral ERM-1/ICB4 overlay (turquoise, arrow) in early-stage mutant (RNAi) phenotype (mt); ICB4 subapical accumulation (blue, arrow) in late-stage mt; same image with separated ICB4 for clarity. (g) NHX-7, a basolateral integral membrane Na+/H+ pump, retained at basolateral membranes, but partially cytoplasmically displaced in late-stage mt. (h) Basolateral LET-413/Scribble, a junction-mediated polarity determinant[59], excluded from apical membrane in wt (no IFB2 overlap) and also from lateralized ectopic lumenal membrane in mt, but not displaced from the basolateral membrane (arrow). **(i – j)** Apical junctions. The junction integrity molecule AJM-1[59] and the adherens junction component HMP-1/alpha-

catenin remain contiguous at apicolateral bounderies in both wt and mt (arrowheads), but additionally surround nascent lateral lumens in mt (arrows; note absence of fragmented junction pattern). **(k)** Feeding of dsRed-labeled bacteria fails to label ectopic lumens (arrows) or the cytoplasm of mt (same sections in all). Confocal images of representative L1 intestinal sections are shown: *pod-2*-, *let-767*-, *acs-1*- and *sptl*-1 RNAi cause the same mis/localization of all markers (N>40 for each marker).

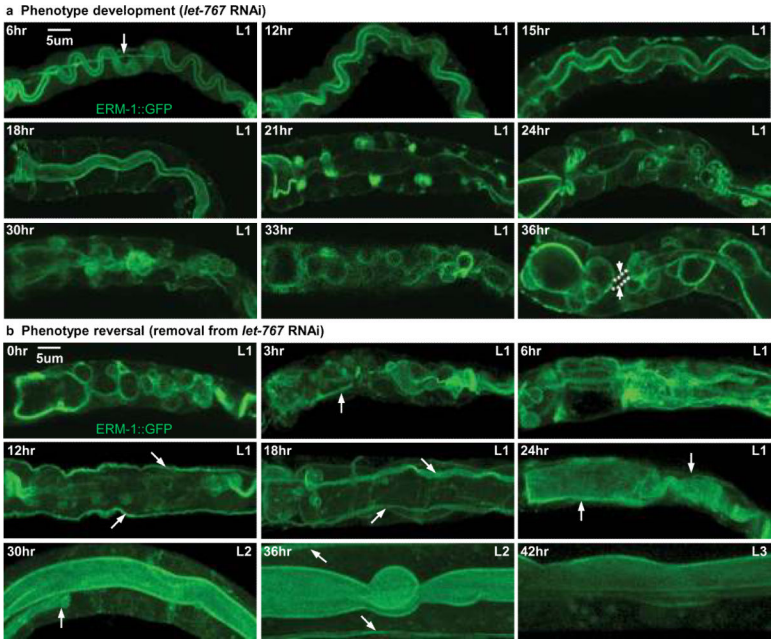

Figure 3. Lipid biosynthesis perturbations reversibly shift apicobasal domain identities and lumen position on expanding intestinal membranes *in situ*

(a) Tracking ERM-1: :GFP dis/placement after lipid-biosynthesis inhibition (0 hour = hatching of *let-767[RNAi]* progeny, not shown): 6hr, apical (excretory canal visible in this image, arrow); 12hr, as puncta in cytoplasm; 15hr, as puncta at basal membranes; 18hr, entire basolateral membranes outlined; 21hr, enriched at apicolateral angle and disappearing from apical membrane; 24hr, at lateral lumens in apicolateral angle; 30hr, at multiple ectopic lumens along lateral membranes; 33hr, at coalescing ectopic lumens; 36hr, at large lateral lumens, almost lost from original apical membrane (arrowheads bracket central lumen area, dotted line indicates missing apical ERM-1: :GFP). **(b)** Tracking ERM-1: :GFP re/placement upon lipid biosynthesis restoration (0 hour = removal from *let-767* RNAi): 0hr, at multiple lateral lumens; 3hr, at smaller lateral lumens; 6hr, at lateral lumens and cytoplasmic; 12hr, cytoplasmic (blurred outlines of small lateral lumens still visible); 18hr, fully cytoplasmic, reappearing at widened contiguous apical membrane (hidden behind excretory canal, arrows); 24hr, at the centering apical/lumenal membrane, lateral lumens no longer visible; 30hr, at the wide central apical membrane and lateral membranes, now without lumens; 36hr, at the fully restored though undulating apical membrane; 42hr, at the apical membrane in the extended epithelium. 42hr-image encompasses 2 INT rings while 0hr-image includes all 9 INT rings: difference reflects epithelial expansion (note stage progression to L2 [30hr] and L3 [42 hr]; compare to L1 arrest 36hr post-RNAi induction [a]). Representative animals are shown, N>200; confocal sections or projections on the level of the intestine: full projections in b to encompass all ERM-1: :GFP; arrows indicate superimposed excretory canals.

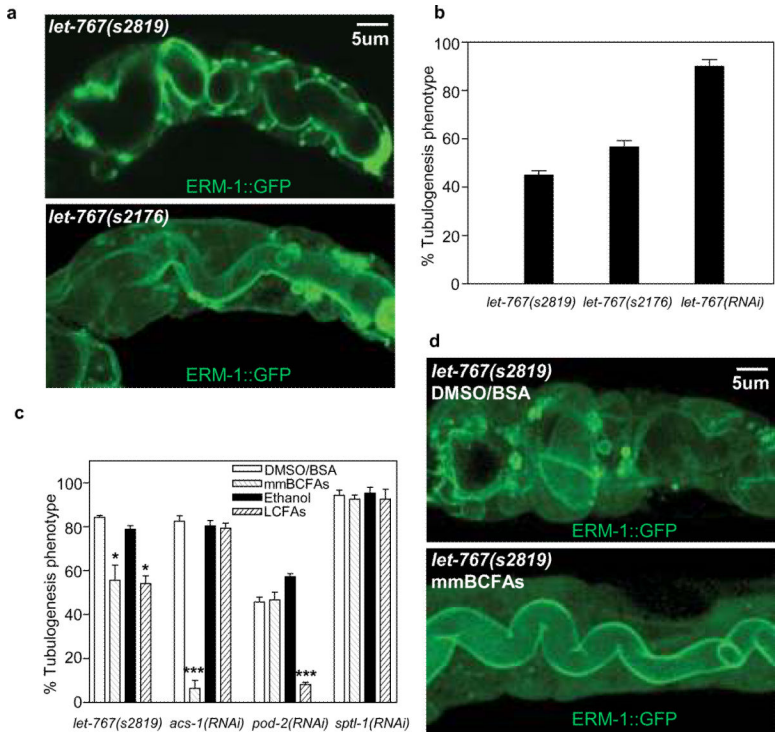

Figure 4. Germline mutations in fatty-acid-biosynthetic enzymes cause intestinal tubulogenesis defects that are rescued with exogenous fatty acids

An allelic series of *let-767* point mutations[26] includes: *s2176*, suggested null (early larval lethality); *s2819*, moderately severe (mid-larval lethality); and *s2464*, less severe allele (reaches adulthood with lethal progeny [maternal-affect]). **(a)** Top - confocal images of: *s2819* with early basolateral ERM-1: :GFP displacement; bottom - *s2176* with early ectopic lumen formation (let-767(s2167/s2819) dpy-17(e164) unc-32(e189)III; sDp3(III;f); fgEx13[perm-1: :erm-1: :gfp rol-6(su1006)]). Lateral ERM-1: :GFP displacement and ectopic lumen formation are obscured in Dpy background with widened intestinal lumen and body shape. **(b)** Penetrance and expressivity of tubulogenesis defects (speed of development and number and size of lateral lumens) increase with allelic severity. Higher penetrance by RNAi than in *s2176* suggests maternal product requirement. All animals evaluated 30hr post-hatching. Mean +/− SD shown, n=5 (N>200 animals per experiment) for mutants and n=5 (N>1000 animals per experiment) for RNAi animals. **(c)** Rescue with exogenous lipids supplied by food. Monomethyl branched chain fatty acids (mmBCFAs) partially rescue *let-767-*, fully rescue *acs-1-*, but not *pod-2(RNAi)* tubulogenesis defects; straight-chain LCFAs partially rescue *let-767-*, fully rescue *pod-2-*, but not *acs-1(RNAi)*. *sptl-1(RNAi)* defects are not rescued with either mmBCFAs or straight-chain LCFAs. Experimental and control animals were evaluated 60hr post-feeding with fatty acids/solvents (Methods). Mean +/− SD is shown, n=5 (N>200 animals per experiment), **P*<0.05 and ****P*<0.001, two-tailed *t* test. **(d)** Top -moderately severe *let-767(s2819)* allele (later stage of phenotype development than in [a]), bottom - almost fully rescued with exogenous mmBCFAs.

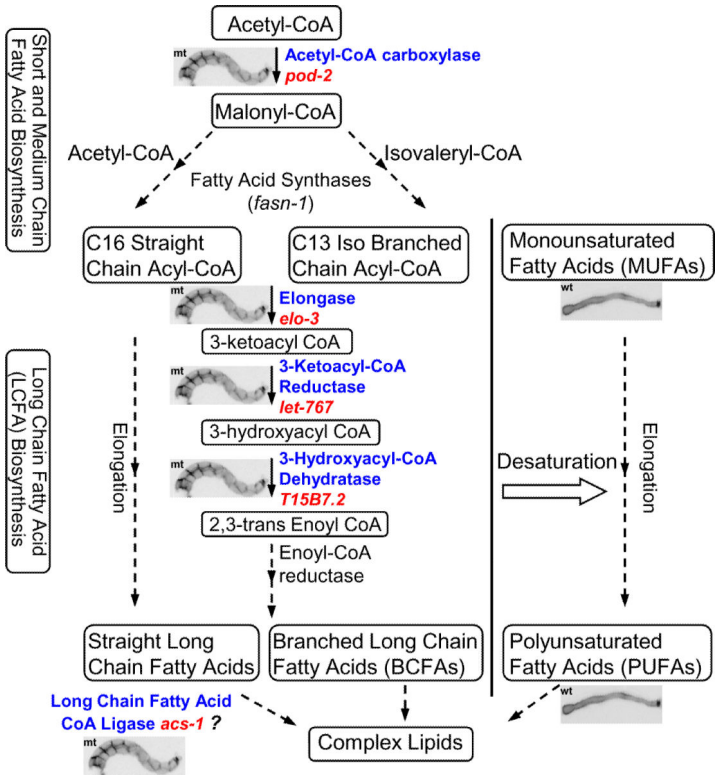

Figure 5. Tubular polarity requires saturated long chain fatty acid (LCFAs) biosynthesis

Conserved fatty-acid-biosynthesis pathways are shown[56]: POD-2/ACC and FASN-1/FAS catalyze the first steps in saturated small and medium chain fatty acid biosynthesis (SFA; top: Acetyl-CoA shown as primer example for even-numbered SFAs, Isovaleryl-CoA for odd-numbered mmBCFAs), subsequently elongated to LCFAs by elongases (middle: this area was probed in greater detail and has been expanded [see text]), variably desaturated by desaturases (right). All products are precursors for complex lipids (bottom). Presence or absence of polarity defects (wild-type [wt] or mutant [mt] indicated throughout by image insets) was evaluated in RNAi animals and/or germline mutants (see Tab.S1 for specific genes targeted [N=162], the majority of which lacked polarity defects; see Fig.S6 for phenotypes). Identified enzymes are shown in blue, corresponding genes in red. *fasn-1(RNAi)* was not identified here due to its early arrest (*pod-2* and *fasn-1* are the only lipid-biosynthetic enzymes previously shown to affect polarity, at the first-cell stage; the mediating lipid compound was not identified[7]). The precise pathway location of *acs-1* is not known. Reducing cholesterol levels to trace amounts did not produce the phenotype (not shown; *C. elegans* is a cholesterol auxotroph, but requires such low amounts of cholesterol that its role as a structural membrane lipid has been questioned[60]).

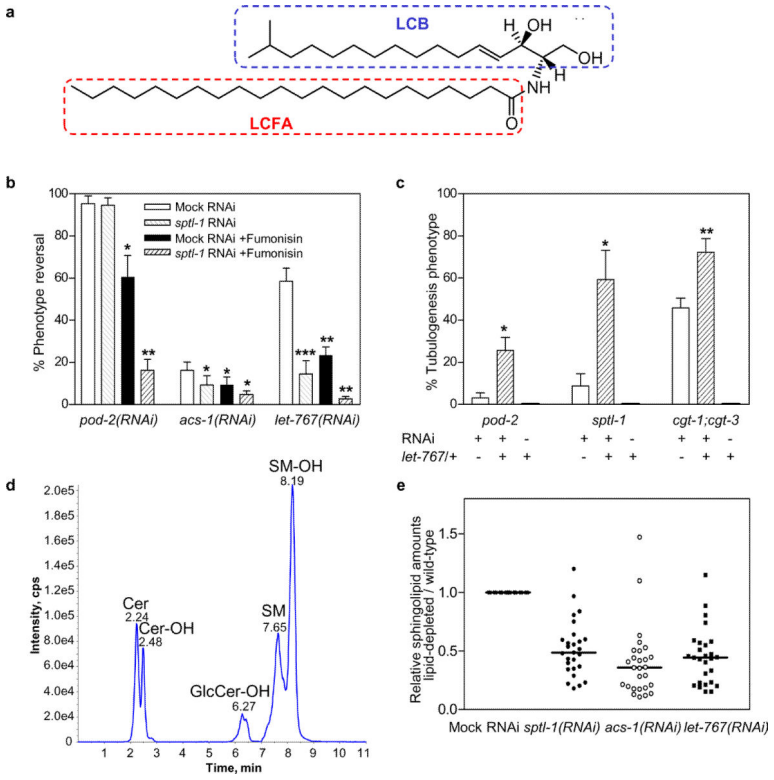

Figure 6. Fatty-acid biosynthesis determines tubular polarity via sphingolipid synthesis

(a) Ceramide: the sphingoid base (LCB) is linked to an LCFA via an amide bond (22:0 hydroxy-15 methyl-2-aminohexadec-4-en-1, 3-diol is shown). **(b)** Reversal of polarity conversion, induced by fatty-acid-biosynthetic-enzyme depletion, requires sphingolipid synthesis. Note: Fumonisin (with and without *sptl-1* RNAi), but not *sptl-1(RNAi)* alone (or Myriocin, not shown), suppresses *pod-2(RNAi)* polarity reversal. Thus POD-2 utilizes LCBs generated during its suppression, suggesting it predominantly generates ceramide LCFAs. Conversely, *acs-1*- and *let-767(RNAi)* polarity reversal is suppressed by *sptl-1* alone, suggesting they lack such LCBs and thus contribute to their synthesis. This is consistent with *let-767*- and *acs-1's* role in mmBCFA-, and *pod-2*- and *let-767's* role in straight LCFA synthesis[23–25] (the LCB requires mmBCFAs[31]) and with the rescue experiments shown in Fig.4B. Conditions of sphingolipid biosynthesis reduction were titrated to prevent induction of the phenotype on their own (Methods; under these conditions, *sptl-1[RNAi]* is enhanced by Fumonisin). For comparison, identical RNAi conditions were used throughout: different reversal efficiencies thus reflect phenotype severity (varies with each enzyme, see Fig.S1,S6; e.g., standard *acs-1* RNAi induces a strong phenotype, less easily reversed). Mean +/− SD is shown, n=4 (N>60 animals per experiment) **P*<0.05, ***P*<0.01 and ****P*<0.001, two-tailed *t* test. **(c)** Dominant genetic interactions between fatty-acid- and sphingolipid-biosynthetic enzymes. *let-767(s2819)*;sDp3 are wild-type, thus any increase of polarity defect it induces in RNAi animals demonstrates enhancement. *pod-2*- and *sptl-1* RNAi were titrated to generate no phenotypes, *cgt-1;cgt-3(RNAi)* was induced at standard conditions. Mean +/− SD is shown, n=5 (N>300 animals per experiment), **P*<0.05, two-tailed *t* test. **(d)** Ion chromatogram of wild-type worm extracts shown for the [M+H]+ m/z 250.3u fragment of their common d17:1 sphingoid base. Interpretation of mass ions from

each peak's mass spectra: 2.24min:d17:1ceramides(Cer), 2.48min:d17:1hydroxyceramides(Cer-OH), 6.27min:d17:1glucosylhydroxyceramides(GlcCer-OH), 7.65min:d17:1sphingomyelins(SM), 8.19min:d17:1 hydroxysphingomyelins(SM-OH). Here and below: synchronized wild-type or enriched RNAi L1s were collected from ~800 plates each (Methods). **(e)** Reduced sphingolipid levels in both sphingolipid- and fatty-acid-biosynthesis-depleted animals. Relative amounts are plotted (C21–26-Cer, -Cer-OH, -GlcCer-OH, C21–23,25-SM and -SM-OH; Tab.S3). Bars indicate median, wild-type arbitrarily set at 1, dots represent individual compounds. Concentrations calculated from the MS-derived response ratio of compound area/internal standard area of the corresponding period per sample dry weight.

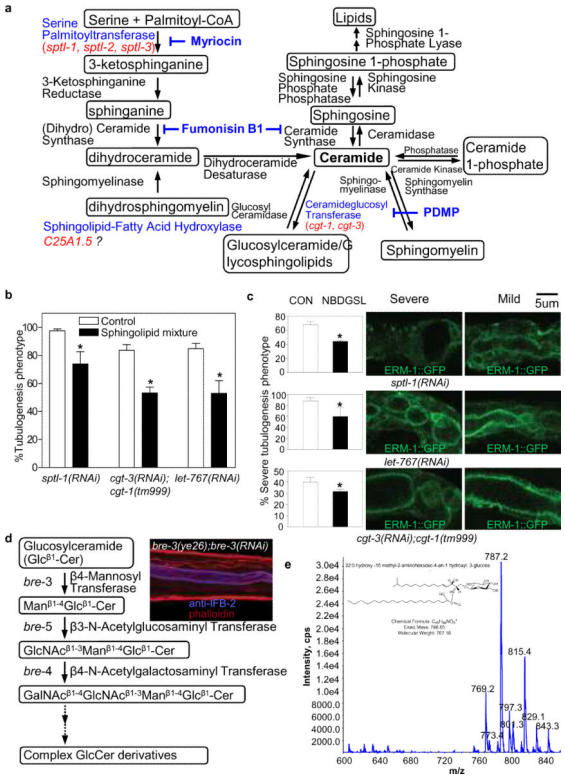

Figure 7. Tubular polarity requires ceramideglycosyltransferases (CGTs) and glycosphingolipids (GSLs)

(a) Conserved sphingolipid metabolic pathways are shown[50]. Left: *de novo* biosynthesis, right: salvage pathway, bottom: complex membrane sphingolipid biosynthesis. Presence/absence of polarity defects were assessed in RNAi animals and/or germline mutants (see Tab.S2 for specific genes targeted [N=85], the majority of which lacked polarity defects; see Fig.S6 for phenotypes). Identified enzymes are shown in blue, corresponding genes in red. Sphingolipid fatty-acid hydroxylase's precise location is unknown. **(b)** *sptl-1-*, *cgt-1(tm999);cgt-3-*, and *let-767(RNAi)* tubulogenesis defects are partially rescued by exogenous sphingolipids. A sphingolipid standard mixture, containing ten different sphingolipid compounds, was fed with RNAi bacteria (Methods). The percentage of animals with tubulogenesis defects was evaluated 64–66 hours after feeding with lipids or solvents (control). Mean +/− SD is shown, n=5 (N>200 animals per experiment) N>1000, **P*<0.05, two-tailed *t* test. **(c)** C6-NBD-GlcCer (NBDGSL) supplementation attenuates ectopic lumen formation in *sptl-1-*, *let-767-* and *cgt-1(tm999);cgt-3-(RNAi)* L1 intestines. Animals were evaluated for `severe' (discontinuous central lumen/large ectopic lumens) versus `mild' (partially contiguous central lumen/small ectopic lumens) phenotypes 5 and 6 days after feeding with GSLs or solvents (CON; supplied with RNAi bacteria). For *sptl-1* RNAi, which induces the strongest phenotype, `severe' was defined as arrest/intestinal disintegration and `mild' as mobile/intestine not disintegrated. Confocal sections of representative animals are shown. Mean +/− SD, n=5 (N>200 animals per experiment), **P*<0.05, two-tailed *t* test. **(d)** The arthro-series of GlcCer-derivatives is dispensable for GlcCer's function in tubular polarity. First steps of insect-type GlcCer-derivative biosynthesis are shown, corresponding *C. elegans* orthologs on left[39]. Inset demonstrates intact intestinal lumen (purple) in the

presumed null allele *bre-3(ye28)* combined with *bre-3(RNAi)* (animals grow to fertile adults)[39]. N>2000. **(e)** Accumulated mass spectra of wild-type GlcCer-OH with elution peak of 6.27min (Fig.6d). GlcCer with m/z 787.2, with a C17 sphingoid base and a hydroxylated saturated C22-fatty-acid chain, was present in greatest abundance (inset). Hydroxyacylamines with saturated C21 (m/z 773.4) and C23–26 carbon chains (m/z 801.3, 815.4, 829.1, and 843.3, respectively) were present in low abundance. Peak m/z 769.2 could represent [M-4H] C21:0-d17:1 and peak m/z 797.3 [M-4H] C23:0-d17:1 GlcCer-OH compounds.

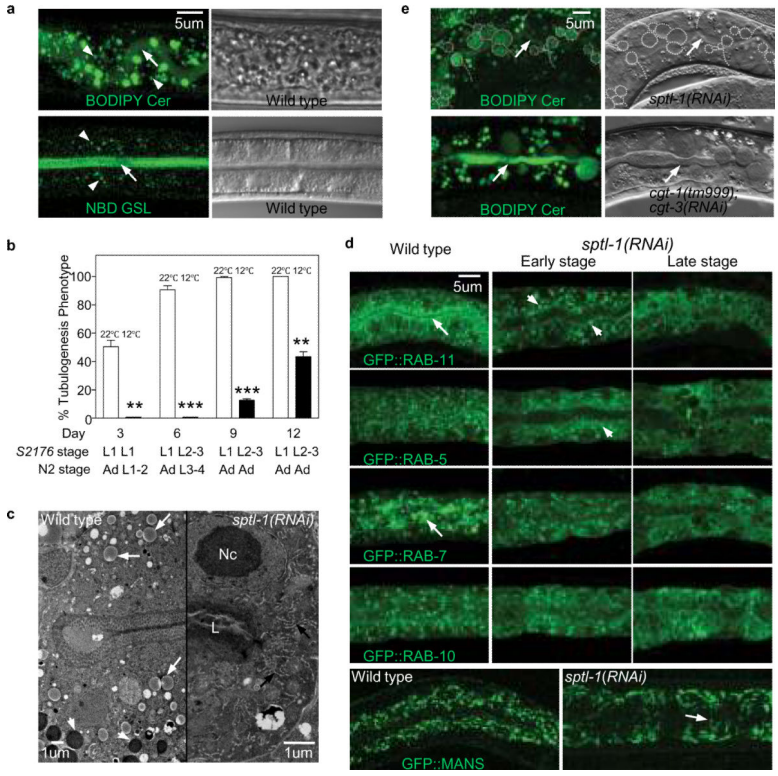

Figure 8. Subcellular localization of exogenous sphingolipids and effects of sphingolipid-biosynthesis suppression on vesicular trafficking

(a) C5-BODIPY-Cer (top) and C6-NBD-GlcCer (NBD-GSL, bottom), supplied with food, localize to intestinal vesicles (arrowheads) and apical/lumenal plasma membranes (arrows) of wild-type animals. Over time, both exogenous lipids accumulate in larger vesicles (NBD-GSL-fed animal is shown immediately after lipid supplementation; Methods). Lumenal membrane lipids are distinguishable from intra-lumenal lipids in NBD-GSL-fed animal. Confocal images shown left and corresponding Nomarski images right. **(b)** Low temperature interference with trafficking[61, 62] inhibits polarity conversion (compare Fig.S8). At 12°C, the *let-767(s2176)* typical moderate polarity defects are suppressed and animals progress beyond L1-arrest to L2/L3. Developmental stages (larval: L1 – 4, adult: Ad) at 12 and 22°C on days 3, 6, 9, 12 post-bleaching shown beneath bars (Methods). Mean +/−SD shown, n=4 (N>120 animals per experiment) ***P*<0.01, ****P*<0.001, two-tailed *t* test. **(c)** TEM L1 intestinal cross sections (Fig.S8 shows whole intestines): vesicle abundance and variety in wild-type (left; including lipid-storage- [arrows] and yolk-vesicles [arrowheads]); vesicle paucity and profusion of distended ER/Golgi membranes (arrow shows example) in *sptl-1(RNAi)* (right; note lumen deformation and missing apical microvilli). L lumen, Nc nucleus. Scale bar, 2 microns. **(d)** Apical endosome populations become depleted during polarity conversion. Left to right shows progression to late-stage polarity defect (representative L1 intestines shown): Lumenal-membrane-associated RAB-11 (arrow) is lost; pancytoplasmic RAB-11-positive vesicles are first mildly enlarged (arrowheads), then mostly lost. Pancytoplasmic RAB-5-positive vesicles are more slowly and less severely depleted (arrowhead indicates occasionally enlarged subapical vesicles). L1-specific subapical RAB-7-positive vesicles aggregates (arrow) are lost; the pancytoplasmic fraction

is unchanged or moderately reduced. Pancytoplasmic RAB-10-positive vesicles are moderately decreased in number. The evenly dispersed vesicular Alpha-mannosidaseII/(MANS)+-Golgi stacks (GFP::MANS) aggregate basolaterally in linear rather than vesicular structures (arrow; compare text). **(e)** C5-BODIPY-Cer displacement to ectopic lateral lumenal membranes in *sptl-1(RNAi)*- (top) and *cgt-1(tm999)/cgt-3(RNAi)* L1 intestines (bottom; confocal images left, corresponding Nomarski images right). Cer-positive ectopic lumenal membranes show lateral membrane connections (outlined by dots [top]) and are distinct from cytoplasmic vesicles; arrows indicate main lumen. All confocal images in this figure are collected at settings limiting autofluorescent vesicle interference.